
Persistent Homology Captures the Generalization of Neural Networks Without A Validation Set

Anonymous Author(s)
Affiliation
Address
email

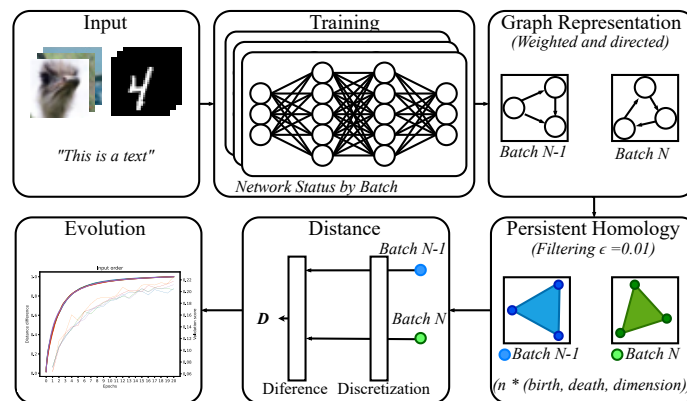


Figure 1: Our proposal.

Abstract

1 The training of neural networks is usually monitored with a validation (holdout)
2 set to estimate the generalization of the model. This is done instead of measuring
3 intrinsic properties of the model to determine whether it is learning appropriately.
4 In this work, we suggest studying the training of neural networks with Algebraic
5 Topology, specifically Persistent Homology (PH). Using simplicial complex repre-
6 sentations of neural networks, we study the PH diagram distance evolution on the
7 neural network learning process with different architectures and several datasets.
8 Results show that the PH diagram distance between consecutive neural network
9 states correlates with the validation accuracy, implying that the generalization error
10 of a neural network could be intrinsically estimated without any holdout set.

11 1 Introduction

12 Generalization is what makes a machine learning model useful; the uncertainty of its behaviour with
13 unseen data is what makes it potentially dangerous. Thus, understanding the generalization error of a
14 model can be considered one of the holy grails of the entire machine learning field.

15 Machine learning practitioners typically monitor some metrics of the model to estimate its generaliza-
16 tion error and stop the training even before the numerical convergence to prevent the overfitting of
17 the model. Usually, the error measure or the metric relevant to the task is computed for a holdout
18 set, the validation set. Since these data have not been directly used for updating the parameters, it
19 is assumed that the performance of the model on the validation set can be used as a proxy of the

20 generalization error, provided it is representative of the data that will be used in inference. One
21 can, though, potentially overfit to this holdout set if it is repeatedly used for guiding a hyperparameter
22 search.

23 Instead of relying on an external set, though, the question of whether it could be possible to estimate
24 the generalization error with some intrinsic property of the model is highly relevant, and it has been
25 barely explored in the literature. On the other hand, Algebraic Topology has recently been gaining
26 momentum as a mathematical tool for studying graphs, machine learning algorithms, and data.

27 In this work, we have the goal of, once having characterized neural networks as weighted, acyclic
28 graphs, represented as Algebraic Topology objects (following previous works), computing distances
29 between consecutive neural network states. More specifically, we can calculate the Persistent
30 Homology (PH) diagram distances between a give state (i.e., when having a specific weights during
31 the training process) and the next one (i.e., after having updated the weights in a training step) (see
32 Figure 1. We observe that during the training procedure of neural networks we can measure this
33 distance in each learning step, and show that there exists a high correlation with the corresponding
34 validation accuracy of the model. We do so in a diverse set of deep learning benchmarks and model
35 hyperparameters. This shines light on the question of whether the generalization error could be
36 estimated from intrinsic properties of the model, and opens the path towards a better theoretical
37 understanding of the dynamics of the training of neural networks.

38 In summary, our contributions are as follows:

- 39 • Based on principles of Algebraic Topology, we propose measuring the distances (Silhouette
40 and Heat) between the PH persistence diagrams obtained from a given state of a neural
41 network during the training procedure and the one in the immediately previous weights
42 update.
- 43 • We empirically show that the evolution of these measures during training correlate with
44 the accuracy in the validation set. We do so in diverse benchmarks (MNIST, CIFAR10,
45 CIFAR100, Reuters text classification), and models (MLPs in MNIST and Reuters, MLPs
46 and CNNs in CIFAR100 and CIFAR100).
- 47 • We thus provide empirical proof of the fact that valuable information related to the learning
48 process of neural networks can be obtained from PH distances between persistence diagrams
49 (*homological convergence*). In particular, we show that homological convergence is related
50 to learning process and the generalization properties of neural networks.
- 51 • In practice, we provide a new tool for monitoring the training of neural networks, and open
52 the path to estimating their generalization error without a validation set.

53 The remainder of this article is as follows. In Section 2 we describe the theoretical background of our
54 proposal in terms of Algebraic Topology, while in Section 3 we go through the related work. Then, in
55 Section 4 we formalize our method. Finally, in sections 6 and 7 we present and discuss our empirical
56 results, respectively.

57 **2 Background**

58 In this section we introduce the mathematical foundations of this paper. A detailed mathematical
59 description is included in the Supplementary Material.

60 A simplicial complex is a set composed of points, line segments, triangles, and their n-dimensional
61 counterparts, named simplex (K). In particular, a simplicial complex must comply with two properties:
62 1. Every face of a simplex is also in the simplicial complex (of lower dimension). 2. The non-empty
63 intersection of any two simplices contained on a simplicial complex is a face of both. 0,1,2,3-simplex
64 and non simplex examples are shown in Figure 2.

65 We can associate to an undirected graph, $G = (V, E)$, a simplicial complex where all the vertices
66 of G are the 0-simplex of the simplicial complex and the complete subgraphs with i vertices, in G
67 corresponds to a $(i - 1)$ -simplex. This type of construction is usually called a complex clique on the
68 graph G , and is denoted by $Cl(G)$. Figure 3 shows a graph clique complex $Cl(G)$ example.

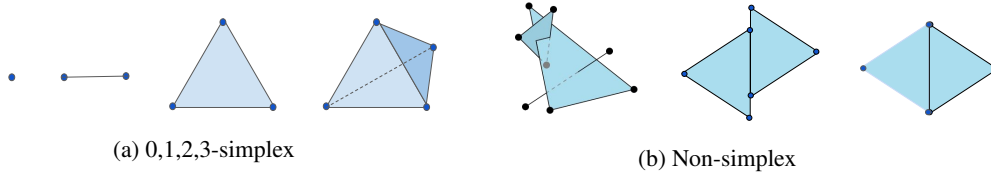


Figure 2: Simplex and non-simplex examples.

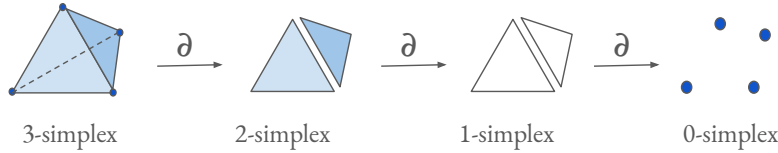


Figure 4: Boundary function sample.

69 The boundary function is defined as a map, from
 70 an i -simplex to an $(i - 1)$ -simplex, as the sum
 71 of its $(i - 1)$ -dimensional faces. A boundary
 72 function sample is shown in Figure 4.

73 In algebraic topology, a k -chain is a combination
 74 of k -simplices (sometimes symbolized as a linear
 75 combination of simplices that compose the
 76 chain). The boundary of a k -chain is a $(k - 1)$ -
 77 chain. It is the linear and signed combination of
 78 chain element boundary simplices. The space of
 79 i -chains is denoted by $C_i(K)$.

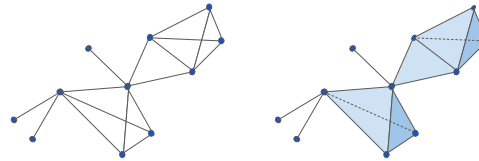


Figure 3: Graph clique complex $Cl(G)$ example.

80 There are two special cases of chains that will be useful to define homology:

- 81 • Closed chain or i -cycle: i -chain with empty boundary. An i -chain c is an i -cycle if and only
 82 if $\partial_i c = 0$, i.e. $c \in \ker(\partial_i)$. This subspace of $C_i(K)$ is denoted as $\mathbb{Z}_i(K)$.
- 83 • Exact chain or i -boundary: An i -chain c is an i -boundary if there exists an $(i + 1)$ -chain
 84 d such that $c = \partial_{i+1}(d)$, i.e. $c \in \text{im}(\partial_{i+1})$. This subspace of $C_i(K)$, the set of all such
 85 i -boundaries forms, is denoted by $\mathbb{B}_i(K)$.

86 Now, if we think in the i -cycles that do not bound an $(i + 1)$ -simplicial complex, this is the definition
 87 i -th homology of the simplicial complex K . The precise definition is the quotient space of $\mathbb{B}_i(K)$ a
 88 subspace of $\mathbb{Z}_i(K)$ (see Supplementary Material). The number of non equivalent i -cycles (Figure 5)
 89 is the dimension of the homology group $H_i(K)$, also named Betti numbers.

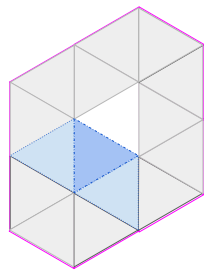


Figure 5: The two blue dashed cycles are homologically equivalent, the pink isn't.

90 We can create a nested family of simplicial complexes,
 91 K_ϵ , where at each step t , K_{ϵ_t} is embedded
 92 in the simplicial complex $K_{\epsilon_{t+1}}$. We call this set
 93 a simplicial complex filtration.

94 For each filtration simplicial complex, we can
 95 calculate the homology groups. Then, we can
 96 look at the birth, that is, when a homology class
 97 appears, and death, the time when the homology
 98 class disappears. The PH treats the birth and the
 99 death of these homological features in K_ϵ for
 100 different ϵ values. The lifespan of each homological
 101 feature can be represented as an interval (*birth, death*),
 102 of the homological class. Given a filtration, this
 103 collection of intervals is named a Persistence Diagram
 104 (PD) [5].

105 It is possible to compare two PDs using specific distances (Wasserstein and Bottleneck). To efficiently
106 perform this operation, due to the size of these diagrams, it is sometimes necessary to simplify them
107 by means of a discretization process (such as Weighted Silhouette and Heat vectorizations).

108 3 Related Work

109 **Algebraic Topology and Machine Learning** The use of Algebraic Topology in the fields of
110 data science and machine learning has been gaining momentum in recent years (see Carlsson [5]).
111 Specifically in the case of neural networks, some works have applied topology for improving the
112 training procedure of the models [15, 8], or pruning the model afterwards [30]. Other works have
113 focused on analyzing the capacity of neural networks [14, 26, 17] or the complexity of input data
114 [17]. Furthermore, recent works have provided topological analysis of the decision boundaries of
115 classifiers based on PH and Betti numbers [24, 22].

116 **Graph and topological representations of neural networks** Gebhart et al. [12] suggest a method
117 for computing the PH over the graphical activation neural networks, while Watanabe and Yamana
118 [29] propose representing neural networks via simplicial complexes based on Taylor decomposition,
119 from which one can compute the PH. Chowdhury et al. [7] show that directed homology can be used
120 to represent MLPs. Anonymous [2] concurrently show neural networks, when represented as directed,
121 acyclic graphs, can be associated to an Algebraic Topology object. By computing the PH diagram,
122 one can effectively characterize neural networks, and even compute distances between two given
123 neural networks, which can be used to measure their similarity. This is unlike other works [11, 13]
124 approximating neural networks representations with regard to the input space.

125 **Estimating the generalization and studying the learning process** We are, though, specifically
126 interested in the use of PH for analyzing the learning process, especially with the goal of estimating
127 generalization. In this regard, the literature is perhaps more limited. Jiang et al. [16] work on
128 understanding what drives generalization in deep networks from a Bayesian of view. Neyshabur et al.
129 [23] study the generalization gap prediction from the training data and network parameters using a
130 margin distribution, which are the distances of training points to the decision boundary. In Li et al.
131 [21], authors propose an alternative to cross-validation for model selection based on training once on
132 the whole train set, without any data split, deriving a validation set with data augmentation.

133 Corneanu et al. [10] try to estimate the performance gap between training and testing using PH
134 measures. They claim. However, one can observe some caveats. The first one is that their regression
135 fitted to predict the test error has a considerably high error, making it not usable in practice. The
136 second caveat is that for fitting the regression one needs at least part of the sequestered testing set.

137 In this work, motivated by the interest of having a better understanding of whether it would be
138 possible to estimate the generalization of neural networks without a holdout set, we suggest using the
139 topological characterization and distances concurrently proposed in Anonymous [2] but, crucially,
140 measured between consecutive weight updates. We will show that the evolution of this distance
141 is similar to the one of the validation accuracy. Unlike Li et al. [21], we do not use any data at
142 all. Unlike [10], we do not build a statistical or machine learning model (linear regression) for
143 predicting the testing error. Instead, we propose a new measure, and we empirically show that it
144 highly correlates with the validation accuracy. Note that in this work we do not work with any input
145 data and activations, but with the parameters of the neural network themselves.

146 4 Approach

147 **Representation** For representing neural networks as graphs, we follow the approach proposed
148 concurrently in Anonymous [2]. We associate to the neural network, at each learning state (defined
149 by its weights), a weighted directed graph that is analyzed as an abstract simplicial complex. It is
150 important to note that abstract simplicial complex are used in opposition to geometric simplicial
151 complex.

152 For every training state, neural network connections are considered as directed and weighted edges
153 between neurons, represented by graph nodes. Biases are considered as new edges that join to isolate
154 vertices. In this representation, activation functions are lost. Bias information could also have been

155 ignored because, as we will see, it is not very informative in terms of homology, but we decided to
156 preserve it.

157 Negative edge weights are represented with reverse edges with the same weight absolute value. We
158 discard the use of weight absolute value as neural networks are not invariant under weight sign
159 transformations. This representation is consistent with the fact that every neuron can be replaced by a
160 neuron from which two edges with opposite weights emerge and converge again on another neuron
161 with opposite weights. From an homological point of view, this would be represented as a closed
162 cycle. Weights are normalized following the Equation 1. ζ is a smoothing parameter that we set to
163 $1e-6$. This smoothing parameter is necessary as we want to avoid normalized weights of edges to be
164 0 (in our representation 0 implies a lack of connection):

$$\max\left(1 - \frac{|w|}{\max(|\max(W)|, |\min(W)|)}, \zeta\right) \quad (1)$$

165 **Algebraic Topology object** For each weighted directed graph associated with the state of a neural
166 network, we link a directed flag complex to it. The topological properties of this directed flag complex
167 are studied using homology groups H_n . We calculate the homology groups up to degree 3 (H_0-H_3).

168 For each state, we use a family of simplicial complexes, K_ε , for a range of values of $\varepsilon \in \mathbb{R}$. The
169 simplicial complex at step ε_t is embedded in the complex at ε_{t+1} , for $\varepsilon_t \leq \varepsilon_{t+1}$, i.e. $K_\varepsilon \subseteq K_{\varepsilon_{t+1}}$. ε
170 is used as a filter that establish the minimum weight of the graph representation edges included on
171 the simplicial complex. This collection of contained simplicial complex (associated to a directed
172 weighted graph), called filtration, $K_{\varepsilon_{min}} \subseteq \dots \subseteq K_{\varepsilon_t} \subseteq K_{\varepsilon_{t+1}} \subseteq \dots \subseteq K_{\varepsilon_{max}}$, where $t \in [0, 1]$ and $\varepsilon_{min} = 0$,
173 $\varepsilon_{max} = 1$ (remember that edge weights are normalized).

174 The sequence of homology groups is calculated by varying the ε parameter to obtain the persistence
175 homology diagram. In our case, persistent homology calculations are performed on \mathbb{Z}_2 . In other
176 words, once the corresponding filter has been applied to the weight of the edges, all connected edges
177 are considered equally.

178 **Distances between persistence diagrams of consecutive states** In this paper, we are interested in
179 comparing PDs between different simplicial complex associated to each training state of the neural
180 network. There are two distances traditionally used to compare PDs, Bottleneck distance (the length
181 of the longest edge) and Wasserstein distance (using the sum of all edges lengths, instead of the
182 maximum). Their stability with respect to perturbations on PDs has been object of different studies
183 [6, 9].

184 In order to make computations feasible and obviate noisy intervals, we filter the PDs by limiting
185 the minimum PD interval size. We do so by setting a minimum threshold $\eta = 0.01$. Intervals with
186 a lifespan under this value are not considered (spurious homological features). Additionally, for
187 computing distances, we need to remove infinity values. As we are only interested in the deaths until
188 the maximum weight value, we replace all the infinity values by 1.0.

189 In our case, our neural networks have millions of persistence intervals per Persistence Diagram,
190 while Wasserstein distance calculations are computationally hard for large PDs. In order to make
191 calculations computationally feasible, we will use a vectorized version of PDs, also called PD
192 discretization. This vectorized version summaries have been proposed and used on recent literature
193 [1, 3, 4, 19, 25]. For persistence diagram distance calculation, we use weighted Silhouette and Heat
194 vectorizations, using the Giotto-TDA library [27].

195 5 Experiments

196 **Data** We validate our method in several heterogeneous (vision, natural language), well-known
197 datasets, namely 1. MNIST [20], 2. CIFAR-10, 3. CIFAR-100 [18], and 4. the Reuters dataset [28]
198 (multi-class and multi-label document classification dataset).

199 **Models** We experiment with two neural architectures, 1. MLPs and 2. CNNs. In the latter case, we
200 use the convolutional layers as a pre-trained model with frozen weights, and we learn an MLP on top
201 of it. The reason we do so is that our method is based in a representation that, at least in the basic
202 form, does not allow capturing information from convolutional layers. Thus, we need a single (exact

203 same weights) feature extractor, to abstract away distances related to the CNN layers and focus on
204 the MLP.

205 **Conducted experiments** We define the *base* MLP architecture as {Input, Linear(512),
206 Dropout(0.2), Linear(512), Dropout(0.2), Output}. In the case of CNNs, the pre-trained
207 model is defined as 3 convolutional blocks with kernel size 3 (starting with 32 channels), interleaved
208 with max pooling (its linear layers are thrown away after the pre-training). On top of the pre-trained
209 CNN, we also define the same base MLP architecture. Then, for each dataset and model (MLP and
210 CNN), we experiment with varying (while keeping the rest fixed to the base architecture)

- 211 1. Layer size (number of units per layer): 4, 16, 32, 128, 256.
- 212 2. Number of labels (the other classes are removed): 2, 4, 6, 8, 10.
- 213 3. Learning rate: 1e-e05, 0.0001, 0.001, 0.01, 0.1
- 214 4. Dropout: 0.0, 0.2, 0.4, 0.5, 0.8.
- 215 5. Input order: 5 random input orders. As a control experiment, for each analyzed problem
216 we run the same configuration with 5 different input orders. If the measured distances are,
217 indeed, related with the learning process of neural networks, these variations should not
218 have any noticeable effect.

219 We run each configuration 5 times with different random seeds (and, thus, weight initializations¹) to
220 see if the results are consistent across runs. All models are trained with the RMSProp optimizer with
221 a batch size of 256.

222 **Distances and validation accuracy computation** Note that homological distances are obtained at
223 the end of each batch, while validation metrics are only computed on each epoch. The methodology
224 we follow to analyze the learning process on each different problem can be summarized with the
225 following steps:

- 226 1. In each training step (i.e., for each batch) we extract the weights from the MLP current state
227 and use them to build an abstract simplicial complex from the associated weighted directed
228 graph.
- 229 2. We calculate the homological persistence diagram of the simplicial complex.
- 230 3. We then calculate the distance between consecutive persistence diagrams (we will call this
231 sequence *homological convergence*). We use two different distances, namely, Heat and
232 Silhouette.
- 233 4. We compare the homological convergence with the evolution of the validation results on
234 neural network learning process.

235 **Hardware** All experiments were executed in a machine with 2 NVIDIA V100 of 32GB, 2 Intel(R)
236 Xeon(R) Platinum 8176 CPU @ 2.10GHz, and of 1.5TB RAM, for a total of around 7 days. We note
237 that our method is considerably demanding in terms of both compute and memory.

238 The code and outputs are fully available in the Supplementary Material under MIT License.

239 6 Results

240 In this section, we highlight the main results, omitting the ones with Silhouette (since the obtained
241 results were clearer with Heat). See the Supplementary Material for the full results (plots and
242 correlations), including the ones with Silhouette distance.

243 We study the relation between the evolution of the PH diagram distances with the one of the validation
244 score with the cumulative values of the distance between homologous persistence diagrams because
245 this value seems much more stable. The information of the distance between the persistence diagrams
246 has been normalized to visualize clearly the type of evolution of each curve on the same scale.
247 Some of the non-normalized plots can be found in the Supplementary Material. Figure 6 shows the
248 cumulative and non-cumulative homology the MNIST experiment with layer size.

¹The pre-trained convolutional weights are always identical, though.

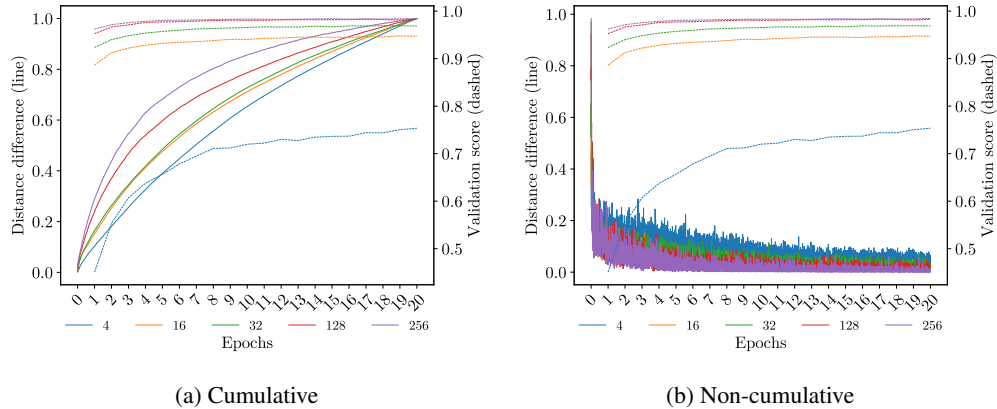


Figure 6: Heat distance and validation accuracy curves on the MNIST experiment with layer size. Normalized.

249 For each experiment (e.g., layer size in MNIST), we plot both the evolution of the PH diagram
 250 distance and the validation score (accuracy). The plotted values are the corresponding means of
 251 the 5 repetitions with different seeds. In addition, we compute the Pearson correlation for these
 252 values. Plots show on the x-axis each training step (for each batch) of the evolution in the training
 253 state of the neural network. On the y-axis, two scales are shown that apply to the distance curves
 254 between accumulated persistence diagrams (solid lines), scale on the right side, and the neural
 255 network validation (dotted lines), numerical scale on the left side. For each sub-experiment (for
 256 example, different values of layer size) a different color was used.

257 The general result is that the evolution of the homological convergence of the MLPs seems to be
 258 very similar to the one of the validation score. This is generally consistent across experiments (see
 259 the Supplementary Material). Table 1 shows the mean (and standard deviations) of the Pearson
 260 correlations for all datasets. All means are above 0.8, implying that there is strong correlation.
 261 Intuitively, this is also observed in the plots, although once the distances are normalized it is not as
 262 clear to visualize. Interestingly, we find that the very few exceptions in which the correlation is low
 263 corresponds to extreme values (very small number of neurons per layer, very high learning rate, very
 264 high dropout), in which the neural network doesn't end up learning properly.

265 In the case of CNNs, the correlations are lower (although still almost always above 0.8 in experiments
 266 such as the one of increasing the number of layers). Recall that in the case of CNN we froze a
 267 single convolutional feature extractor, since our method only supports MLPs. We believe these lower
 268 correlations can be explained because an important part of the learning process happened in the
 269 convolutional layers (in the pre-training), which we do not capture.

270 Another finding is that the method obtains consistent results across runs, meaning that it is capturing
 271 information related to important properties of the networks themselves instead of random artifacts.

272 When varying the studied hyperparameters, we observe that the curves for each configuration are
 273 indeed, different. Remarkably, in the control experiments, this is not the case; results show that the
 274 homological convergence during the learning of the same problem with the same model but with
 275 different input order is very similar. The alteration of the order of the input doesn't have any effect in
 276 the homological convergence. The results of two of these experiments are shown in Figure 7.

277 In addition, we observe that when the neural network learns the given problem, homological conver-
 278 gence occurs. For example, when the layer size is modified, the capacity of the neural network to
 279 learn the problem changes (Figure 6). When it can't learn the problem, because the network does not
 280 have sufficient capacity (the layer size is too small, 4 units), the homology does not seem to converge.

281 Regarding the learning rate, the results are coherent with the intuition that it is a fundamental
 282 parameter that controls how much to change the model in response to the estimated error during the
 283 learning process. A too small learning rate may result in a long training process that could be stalled,
 284 while a too large value may fall in a fast suboptimal solution or an unstable training process. Using
 285 homological convergence we find similar behaviour, as can be seen in Figure 9.

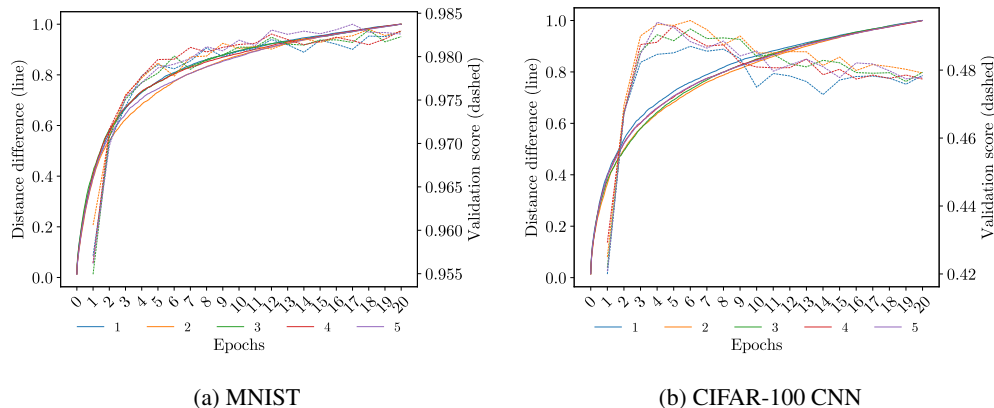


Figure 7: Learning evolution on input order experiments (control experiments). Normalized.

Dataset	Heat distance		Silhouette distance	
	Means mean	Deviations mean	Means mean	Deviations mean
MNIST	0.8910	0.0424	0.8910	0.0424
Reuters	0.6220	0.0700	0.6220	0.0700
CIFAR-10 MLP	0.8233	0.0649	0.8233	0.0649
CIFAR-10 CNN	0.4241	0.1915	0.4241	0.1915
CIFAR-100 MLP	0.8420	0.0566	0.8420	0.0566
CIFAR-100 CNN	0.6130	0.0800	0.6130	0.0800

Table 1: Correlation of validation values with topological difference cumulative. Correlation is computed with 20 points.

286 Finally, we note that even if the two convergences (validation and homological convergence) are
 287 correlated, they are not the same process. This is especially visible in the case of the learning rate
 288 experiments. For instance, in Figure 9, homological convergence is reached before the stabilization of
 289 the validation accuracy. Presumably, they are not capturing the exact same information; specifically,
 290 we believe that the difference is due to the fact that the validation accuracy depends on the specifics
 291 of the data sampled in the validation subset, while the homological convergence is independent of the
 292 validation data.

293 7 Discussion

294 We posed the of question whether homological convergence (in terms of distances between PH
 295 diagrams in consecutive neural network states) is related to the learning process of neural networks.
 296 We have seen that, indeed, it is the case, with strong empirical results backing our claim.

297 This finding has a remarkable implication. If the homological convergence evolution mirrors the
 298 validation accuracy curve, one could ignore the validation set to monitor the training. This opens the
 299 path towards estimating the generalization of neural networks without the need of any holdout set.
 300 Researchers have wondered for a long time whether generalization could be predicted from intrinsic
 301 properties of the model or training data alone (i.e., without a holdout set), and in fact our works
 302 have claimed to do so. Although we do not provide any predictive model, we show that our proposed
 303 measures strongly correlate with the validation accuracy. In addition, we do so by not using any data
 304 at all; we just look at the neural network itself.

305 Our contribution aims pushing towards having a better understanding of the learning process of neural
 306 networks, not targeting any specific direct application. However, we note that it can be effectively
 307 used for monitoring the training of neural networks in terms of convergence expected generalization,
 308 as we have extensively shown in the experiments. Apart from the cases without access to a validation

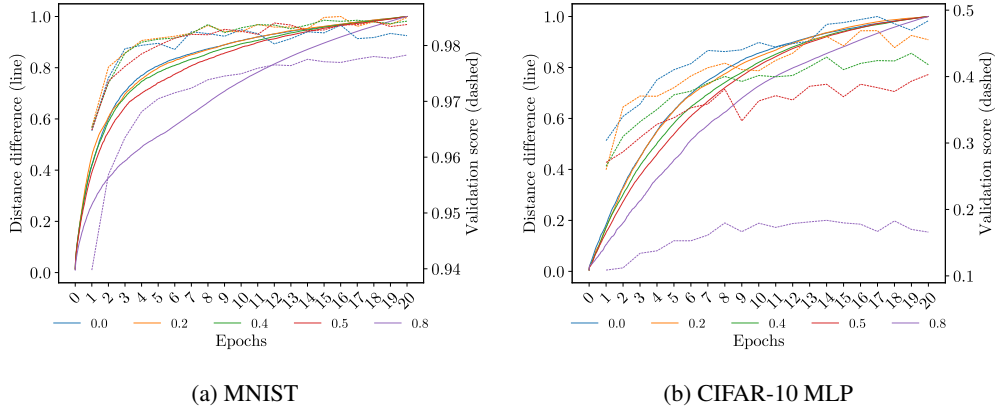


Figure 8: Learning evolution when dropout parameter is changed. Normalized.

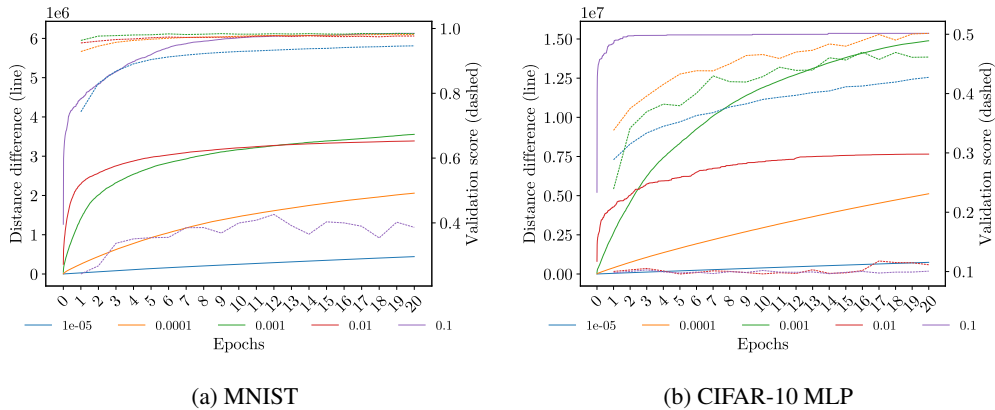


Figure 9: Learning evolution when modifying the learning rate parameter. Not normalized.

309 set, this is relevant because depending on a validation set has the risk of overfitting to it. Having an
 310 intrinsic, well-principled measure should be more robust to random noise in a specific data sample.

311 The main limitation of our method is its computational scalability. As we said in Section 5, our
 312 method took more than 7 days of compute in a HPC machine, even if we restricted the experiments
 313 to small datasets and parameter count. However, we note that our approach computes the *exact*
 314 persistence diagram distances, that is, we do not simplify the graph representation of the neural
 315 networks (we keep every single neuron and connections) and we do not approximate any computation.
 316 This leaves room for finding efficient approximations, opening a new research line. In addition, this
 317 lack of scalability has prevented us from validating our method on bigger models and datasets.

318 Finally, we note that instead of computing correlations, serving as a basic quantitative study, it would
 319 be interesting to perform a time-series analysis to gain more insights on how the two curves vary
 320 together. Moreover, it would have been interesting to investigate how to build a predictive model of
 321 the validation accuracy from the PH distances, but it is was of the scope of this work.

322 8 Conclusions & Future Work

323 In this work, we have provided an empirical proof of the fact that homological convergence is related
 324 to the learning process and generalization properties of neural networks. Furthermore, we have
 325 shown that it can be used to monitor the training of a neural network (and potentially estimating its
 326 generalization) without a validation set. As future work, we suggest generalizing our representation
 327 to other neural architectures and scaling up the experiments to larger models and datasets, for which
 328 finding efficient approximations of our method will be crucial.

329 **Checklist**

- 330 1. For all authors...
- 331 (a) Do the main claims made in the abstract and introduction accurately reflect the paper's
332 contributions and scope? [Yes]
- 333 (b) Did you describe the limitations of your work? [Yes] See the Discussion Section.
- 334 (c) Did you discuss any potential negative societal impacts of your work? [N/A]
- 335 (d) Have you read the ethics review guidelines and ensured that your paper conforms to
336 them? [Yes]
- 337 2. If you are including theoretical results...
- 338 (a) Did you state the full set of assumptions of all theoretical results? [N/A]
- 339 (b) Did you include complete proofs of all theoretical results? [N/A]
- 340 3. If you ran experiments...
- 341 (a) Did you include the code, data, and instructions needed to reproduce the main experi-
342 mental results (either in the supplemental material or as a URL)? [Yes] Both code and
343 outputs.
- 344 (b) Did you specify all the training details (e.g., data splits, hyperparameters, how they
345 were chosen)? [Yes] Check the Experiments Section and the code.
- 346 (c) Did you report error bars (e.g., with respect to the random seed after running ex-
347 periments multiple times)? [Yes] We include means, standard deviations and raw
348 outputs.
- 349 (d) Did you include the total amount of compute and the type of resources used (e.g., type
350 of GPUs, internal cluster, or cloud provider)? [Yes] Check Experiments Section.
- 351 4. If you are using existing assets (e.g., code, data, models) or curating/releasing new assets...
- 352 (a) If your work uses existing assets, did you cite the creators? [Yes] In the case of the
353 datasets. We do not use any other additional asset.
- 354 (b) Did you mention the license of the assets? [No]
- 355 (c) Did you include any new assets either in the supplemental material or as a URL? [Yes]
356 Code, results and pictures we have made for explanations.
- 357 (d) Did you discuss whether and how consent was obtained from people whose data you're
358 using/curating? [N/A]
- 359 (e) Did you discuss whether the data you are using/curating contains personally identifiable
360 information or offensive content? [N/A]
- 361 5. If you used crowdsourcing or conducted research with human subjects...
- 362 (a) Did you include the full text of instructions given to participants and screenshots, if
363 applicable? [N/A]
- 364 (b) Did you describe any potential participant risks, with links to Institutional Review
365 Board (IRB) approvals, if applicable? [N/A]
- 366 (c) Did you include the estimated hourly wage paid to participants and the total amount
367 spent on participant compensation? [N/A]

368 **References**

- 369 [1] H. Adams, T. Emerson, M. Kirby, R. Neville, C. Peterson, P. Shipman, S. Chepushtanova,
370 E. Hanson, F. Motta, and L. Ziegelmeier. Persistence images: A stable vector representation of
371 persistent homology. *J. Mach. Learn. Res.*, 18:8:1–8:35, 2017.
- 372 [2] A. Anonymous. Characterizing and measuring the similarity of neural networks with persistent
373 homology, 2021.
- 374 [3] E. Berry, Y.-C. Chen, J. Cisewski-Kehe, and B. T. Fasy. Functional summaries of persistence
375 diagrams. *Journal of Applied and Computational Topology*, 4:211–262, 2020.
- 376 [4] P. Bubenik. Statistical topological data analysis using persistence landscapes. *J. Mach. Learn.
377 Res.*, 16:77–102, 2015.
- 378 [5] G. Carlsson. Topology and data. *Bulletin of the American Mathematical Society*, 46:255–308,
379 2009.
- 380 [6] F. Chazal, V. D. Silva, and S. Oudot. Persistence stability for geometric complexes. *Geometriae
381 Dedicata*, 173:193–214, 2012.
- 382 [7] S. Chowdhury, T. Gebhart, S. Huntsman, and M. Yutin. Path homologies of deep feedforward
383 networks. *2019 18th IEEE International Conference On Machine Learning And Applications
384 (ICMLA)*, pages 1077–1082, 2019.
- 385 [8] J. Clough, I. Öksüz, N. Byrne, V. Zimmer, J. A. Schnabel, and A. P. King. A topological
386 loss function for deep-learning based image segmentation using persistent homology. *IEEE
387 transactions on pattern analysis and machine intelligence*, PP, 2020.
- 388 [9] D. Cohen-Steiner, H. Edelsbrunner, and J. Harer. Stability of persistence diagrams. *Proceedings
389 of the twenty-first annual symposium on Computational geometry*, 2005.
- 390 [10] C. Corneanu, M. Madadi, S. Escalera, and A. Martínez. Computing the testing error without a
391 testing set. *2020 IEEE/CVF Conference on Computer Vision and Pattern Recognition (CVPR)*,
392 pages 2674–2682, 2020.
- 393 [11] C. A. Corneanu, M. Madadi, S. Escalera, and A. M. Martinez. What does it mean to learn in
394 deep networks? and, how does one detect adversarial attacks? In *2019 IEEE/CVF Conference
395 on Computer Vision and Pattern Recognition (CVPR)*, pages 4752–4761, 2019. doi: 10.1109/
396 CVPR.2019.00489.
- 397 [12] T. Gebhart, P. Schrater, and A. Hylton. Characterizing the shape of activation space in deep neu-
398 ral networks. *2019 18th IEEE International Conference On Machine Learning And Applications
399 (ICMLA)*, pages 1537–1542, 2019.
- 400 [13] W. H. Guss and R. Salakhutdinov. On characterizing the capacity of neural networks using
401 algebraic topology. *CoRR*, abs/1802.04443, 2018. URL [http://arxiv.org/abs/1802.
402 04443](http://arxiv.org/abs/1802.04443).
- 403 [14] W. H. Guss and R. Salakhutdinov. On characterizing the capacity of neural networks using
404 algebraic topology. *ArXiv*, abs/1802.04443, 2018.
- 405 [15] C. Hofer, F. Graf, M. Niethammer, and R. Kwitt. Topologically densified distributions. *ArXiv*,
406 abs/2002.04805, 2020.
- 407 [16] Y. Jiang, D. Krishnan, H. Mobahi, and S. Bengio. Predicting the generalization gap in deep
408 networks with margin distributions. *ArXiv*, abs/1810.00113, 2019.
- 409 [17] E. Konuk and K. Smith. An empirical study of the relation between network architecture and
410 complexity. *2019 IEEE/CVF International Conference on Computer Vision Workshop (ICCVW)*,
411 pages 4597–4599, 2019.
- 412 [18] A. Krizhevsky. Learning multiple layers of features from tiny images. 2009.
- 413 [19] P. Lawson, A. Sholl, J. Brown, B. T. Fasy, and C. Wenk. Persistent homology for the quantitative
414 evaluation of architectural features in prostate cancer histology. *Scientific Reports*, 9, 2019.
- 415 [20] Y. LeCun and C. Cortes. MNIST handwritten digit database. 2010. URL [http://yann.lecun.
416 com/exdb/mnist/](http://yann.lecun.com/exdb/mnist/).
- 417 [21] W. Li, C. Geng, and S. Chen. Leave zero out: Towards a no-cross-validation approach for model
418 selection. *CoRR*, abs/2012.13309, 2020. URL <https://arxiv.org/abs/2012.13309>.

- 419 [22] G. Naitzat, A. Zhitnikov, and L. Lim. Topology of deep neural networks. *J. Mach. Learn. Res.*,
420 21:184:1–184:40, 2020.
- 421 [23] B. Neyshabur, S. Bhojanapalli, D. McAllester, and N. Srebro. Exploring generalization in deep
422 learning. In *NIPS*, 2017.
- 423 [24] K. Ramamurthy, K. R. Varshney, and K. Mody. Topological data analysis of decision boundaries
424 with application to model selection. *ArXiv*, abs/1805.09949, 2019.
- 425 [25] B. A. Rieck, F. Sadlo, and H. Leitte. Topological machine learning with persistence indicator
426 functions. *ArXiv*, abs/1907.13496, 2019.
- 427 [26] B. A. Rieck, M. Togninalli, C. Bock, M. Moor, M. Horn, T. Gumbsch, and K. Borgwardt.
428 Neural persistence: A complexity measure for deep neural networks using algebraic topology.
429 *ArXiv*, abs/1812.09764, 2019.
- 430 [27] G. Tauzin, U. Lupo, L. Tunstall, J. B. Pérez, M. Caorsi, A. Medina-Mardones, A. Dassatti,
431 and K. Hess. giotto-tda: A topological data analysis toolkit for machine learning and data
432 exploration, 2020.
- 433 [28] M. Thoma. The reuters dataset, July 2017. URL [https://martin-thoma.com/
434 nlp-reuters](https://martin-thoma.com/nlp-reuters).
- 435 [29] S. Watanabe and H. Yamana. Topological measurement of deep neural networks using persistent
436 homology. In *ISAIM*, 2020.
- 437 [30] S. Watanabe and H. Yamana. Deep neural network pruning using persistent homology. In *2020
438 IEEE Third International Conference on Artificial Intelligence and Knowledge Engineering
439 (AIKE)*, pages 153–156. IEEE, 2020.